Bit-Error Bounds for Trellis-Coded MPSK in Mixed Fading Channels

Wen-Chang Lin and Yu T. Su, *Member, IEEE*

***Abstract*—Bit-error probability (BEP) bounds of trellis-coded MPSK systems over two classes of mixed fading channels are studied. These two classes of channels have been proposed as candidate models for mobile satellite communications. The first class consists of slow and frequency-nonselective fading channels whose output field strengths follow a probability law characterized by a convex combination of Rician and Rayleigh/lognormal distributions. For the other class of fading channels, the received signal amplitude has a convex combination of Rician and Rician/lognormal distributions. We analyze performance bounds for trellis codes that belong to the class of either geometrically uniform codes (GUC's) or quasi-regular codes (QRC's). Receivers with either ideal channel state information (CSI) or no CSI at all are considered. We examine asymptotic behaviors of these codes and identify key design parameters. Numerical results are provided to illustrate and compare the BEP performances of various codes and to validate the usefulness of the asymptotic analysis.**

***Index Terms*—Fading channels, satellite communication, trellis-coded modulation.**

I. Introduction

LAND MOBILE satellite communication systems have emerged in recent years as an alternative to complement terrestrial mobile radio systems and to provide new services previously unavailable to land mobile users. As pointed out in [1], the constraint on the downlink flux density and the requirement of a small receiving antenna aperture make a mobile satellite channel power limited. On the other hand, to serve a large number of users in a given bandwidth, it is inevitably band limited. For such an operation scenario, trellis-coded modulation (TCM) is a good candidate modulation scheme [1], [2] for it is both power and bandwidth efficient.

Experiments had been conducted to measure and model mobile satellite communication channels [3]–[6]. In cases where a line-of-sight (LOS) path is available, e.g., when the mobile is in an open terrain, the received signal amplitude is generally modeled as a Rician random variable (r.v.) [1]. Measurement results also indicated that multipath and shadowing effects cause the mean received signal strength to vary with the receiver location, and this mean strength can be described by a lognormal distribution [7]–[9]. Loo [5] proposed a model, which assumes that the LOS component under foilage shadowing follows a lognormal distribution. The resulting signal strength has a combined Rician/lognormal (shadowed Rician) distribution. These propagation models are suitable for approximating short-term signal strength variations only. Two different approaches have been adopted to account for both short- (or small area) and long-term (or large area) fading effects in a mobile satellite environment. The first approach assumes that the overall signal strength statistic follows a convex combination of a Rician probability density function (pdf) and a Rayleigh/lognormal pdf [4]. Another approach [6] uses a combination of a Rician r.v. and a Rician/lognormal r.v. to model the received field strength. Both approaches use a parameter called time-share factor or fraction of shadowing, denoted by $A, 0 \leq A \leq 1$, to account for the mobile environment in which the downlink receiver has a LOS view of the satellite with a probability of $1 - A$.

Performance bounds for a two-state TCM signal on a Rician fading channel was presented by Divsalar and Simon [11]. Mckay *et al*. [2] evaluated performance bounds for a four-state TCM system on both Rician and shadowed Rician channels. Benedetto *et al*. [13] have divided various TCM schemes into four classes. Ordered in increasing degrees of symmetry, they are called general codes (GC's), quasi-regular codes (QRC's), regular codes, and geometrically uniform codes (GUC's). The code studied in [11] belongs to the class of GUC, while that in [2] is a member of QRC. This paper extends the works of [2] and [11] to the cases characterized by the two mixed channel models mentioned above. These two classes encompass a large fraction of mobile satellite communication channels encountered in practice. Using appropriate values for the related channel parameters, we can accurately describe the communication environment under investigation. TCM performance bounds in a mixed channel characterized by Barts and Stutzman [6] can be obtained from [2] by straightforward extension and suitable combinations. But our derivations of those in the other class of mixed channels are new. Furthermore, we present asymptotical analysis for both classes and obtain results that are similar to that shown in [1]. The rest of this paper is organized as follows. The next section provides an equivalent baseband block diagram of the system and two probabilistic models of the mobile satellite channels to be studied. The basic analysis technique used in [2] and [11], which is the starting point of our derivation, is also briefly reviewed there. The associated bit-error probability (BEP) bounds are derived in Section III. Section IV analyzes the asymptotic behaviors under various operation scenarios. Section V presents numerical results of our analysis, and in the last section, the major results are summarized.

Manuscript received May 6, 1995; revised August 10, 1995. Part of this paper was presented at the International Symposium on Communications, Dec. 27–29, 1995, Taipei, Taiwan. This work was supported by the National Science Council of Taiwan under Grant NSC84-2612-E009-003.

The authors are with the Department of Communication Engineering, National Chiao Tung University, Hsinchu 30049, Taiwan.

Publisher Item Identifier S 0018-9545(97)05120-7.

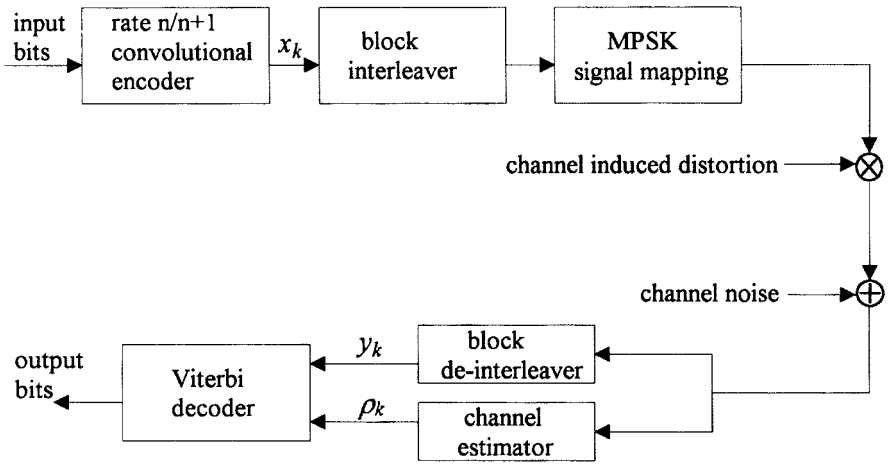

Fig. 1. Baseband model for a trellis-coded MPSK system.

II. System and Channel Models and Performance Bounds

A. Baseband System Model

An equivalent baseband block diagram for the system under investigation is shown in Fig. 1. The data stream enters a rate $n/n+1$ binary convolutional encoder. The encoder output symbols are then block interleaved and mapped into an MPSK signal according to a predetermined set partitioning rule [1]. The transmitted signals are impaired by amplitude/phase distortions and additive white Gaussian noise. The received samples are deinterleaved before being fed into the Viterbi convolutional decoder. CSI can be derived from the received waveform to help the convolutional decoder in improving its performance. Of course, the decoding metric used when CSI is available is different from that without CSI. Subsequent discussion, like the analysis presented in [2] and [11], assumes: 1) interleaving and deinterleaving is such that the "channel" between the interleaver and deinterleaver is memoryless; 2) the communication channel suffers from slow and frequency-nonselective fading; 3) perfect coherent detection is achieved; and 4) an infinite decoding delay in the Viterbi decoding process.

B. Channel Models

Two classes of channel models are considered. The first class models the received signal power as a r.v. whose pdf is a convex combination of Rician and Rayleigh/lognormal distributions [4]

$$P(S) = (1-A)P_{\text{Rice}}(2S; c_0/2S, 1, 2\sqrt{S}) + A\int_0^\infty P_{\text{Ray}}(S|S_0)P_{\text{Ln}}(S_0; 2\mu_0, 2\sigma)\,dS_0 \quad (1)$$

where c_0 in the Rician part represents the direct to multipath signal power ratio

$$P_{\text{Rice}}(x; a, b, c) = ab^2x\exp[-a(b^2x^2+c^2)/2] \times I_0(abcx) \quad (2a)$$

$$P_{\text{Ray}}(S|S_0) = \frac{1}{S_0}\exp(-S/S_0) \quad (2b)$$

$$P_{\text{Ln}}(x; a, b) = \frac{20}{b\ln 10\sqrt{2\pi}x} \times \exp\left[-\frac{(20\log x - a)^2}{2b^2}\right]. \quad (2c)$$

This model degenerates to a pure Rician fading model when $A = 0$. For this special case, we have a more compact expression

$$P(S) = P_{\text{Rice}}(2S; c_0/2S, 1, 2\sqrt{S}) = c_0\exp[-c_0(S+1)]I_0(2c_0\sqrt{S}). \quad (3)$$

Furthermore, it becomes a Rayleigh fading channel if we make the change of variable $S^2 = x^2(1+c_0/c_0)$ and set both A and c_0 to zero.

The Barts and Stutzman model [6] is the second class of interest. In this model, the received amplitude's pdf is given by

$$P(v) = (1-A)P_{\text{Rice}}(v; k, 1, \sqrt{2}) + A\int_0^\infty P_{\text{Rice}}(v; \overline{k}, 1, z)P_{\text{Ln}}(z; m, b_0)\,dz. \quad (4)$$

This model reduces to the one proposed by Loo [5] when $A = 1$. For convenience of comparison, we use normalizations such that the mean-squared value of the received signal amplitude equals one. This can be accomplished by letting $S = h_1^2\rho_1^2$ and $v = \rho_2 h_2$, where

$$h_1 = \sqrt{(1-A)h_{11} + Ah_{12}} \quad (5a)$$

$$h_2 = \sqrt{(1-A)h_{21} + Ah_{22}} \quad (5b)$$

$$h_{11} = \frac{1+c_0}{c_0}$$

$$h_{12} = \exp\left[\frac{\sigma^2}{2}\left(\frac{\ln 10}{10}\right)^2 + \mu_0\frac{\ln 10}{10}\right]$$

$$h_{21} = \frac{2}{k}(1+k)$$

$$h_{22} = \frac{2}{\overline{k}} + \exp\left(\frac{b_0^2}{2}\left(\frac{\ln 10}{10}\right)^2 + m\frac{\ln 10}{10}\right).$$

The pdf's for the normalized amplitudes corresponding to (1) and (4) become

$$P_1(\rho_1) = (1-A)P_{\text{Rice}}(\rho_1; 2c_0, h_1, 1) + A(2h_1^2\rho_1)\int_0^\infty P_{\text{Ray}}(h_1^2\rho_1^2|S_0)P_{\text{Ln}}(S_0; 2\mu_0, 2\sigma) \cdot dS_0 \tag{6a}$$

and

$$P_2(\rho_2) = (1-A)P_{\text{Rice}}(\rho_2; k, h_2, \sqrt{2}) + Ah_2\int_0^\infty P_{\text{Rice}}(\rho_2; \overline{k}, h_2, z)P_{\text{Ln}}(z; m, b_0)\,dz. \tag{6b}$$

An advantage of such normalizations can be noticed by comparing the Rician parts of (1) and (6a). Now there is only one parameter in (6a) that has to do with the random amplitude, while there are three in (1). Note that in normalizing the Rician parts of (1) and (4), we have invoked the identity

$$J_1(h,x,y) \stackrel{\text{def}}{=} \int_0^\infty z^3 x h^2 \exp\left[-\frac{x(h^2z^2+y^2)}{2}\right] I_0(xhyz)\,dz = \frac{2}{xh^2}(1+xy^2/2) \tag{7}$$

which can easily be derived from [14, (11.4.28) and (13.1.27)].

C. BEP Performance

This section gives a brief review of the basic analysis procedure used in evaluating the BEP bound of a TCM system. For more detailed presentation, readers may refer to [1] and [13]. Let the coded sequence be $\underline{x} = (x_1, x_2, \cdots, x_l)$, where x_k's are complex numbers representing the MPSK signals. At the receiving end, the deinterleaved sample sequence can be expressed as $\underline{y} = (y_1, y_2, \cdots, y_l)$, where

$$y_k = \rho_k x_k + n_k \tag{8}$$

ρ_k is a real r.v. representing the effect of channel fading on the received amplitude and n_k is an additive complex Gaussian r.v. with zero mean and variances σ^2. Note that as a result of the perfect coherent detection assumption, phase distortion does not appear in (8). Furthermore, the perfect interleaving/deinterleaving assumption makes all $\rho_k, k = 1, 2, \cdots, n$ independent. The probability that $\underline{x}'$ is the decoded sequence, while $\underline{x} \neq \underline{x}'$ is the transmitted sequence, denoted $P(\underline{x} \to \underline{x}')$, is

$$P(\underline{x} \to \underline{x}') = P_r(m(\underline{y}, \underline{x}') \geq m(\underline{y}, \underline{x})|\underline{x}) \tag{9}$$

where

$$m(\underline{y}, \underline{x}) = \sum_{k=1}^{l} m(y_k, x_k) \tag{10}$$

and

$$m(y_k, x_k) = \begin{cases} -|y_k - \rho_k x_k|^2, & \text{with ideal CSI} \\ -|y_k - x_k|^2, & \text{without CSI} \end{cases} \tag{11}$$

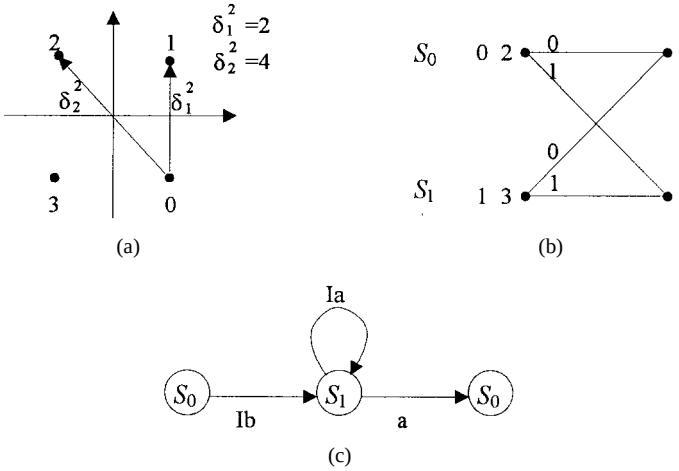

Fig. 2. (a) Signal constellation and squared Euclidean distance of a two-state rate 1\2 4PSK code. (b) The trellis diagram. (c) The corresponding signal flow graph.

is the decoding metric. The BEP, denoted P_b, can then be upperbounded by [13]

$$P_b \leq \frac{1}{2n}\sum_{\underline{x}} P(\underline{x}) \sum_{\underline{x}'} a(\underline{x}, \underline{x}')P(\underline{x} \to \underline{x}') \tag{12}$$

where $a(\underline{x}, \underline{x}')$ is the Hamming distance between $\underline{x}$ and $\underline{x}'$ and both summations are performed over all possible code words (of all lengths). Furthermore, if we denote $\overline{E}_b$ as the average bit signal energy, N_0 the one-sided noise power spectral density, η the set of all k's for which the corresponding kth transmitted symbol x_k is incorrectly decoded (i.e., $x_k \neq x_k'$), and let λ be a nonnegative number, we can show [11] that the pairwise error probability is bounded by

$$P(\underline{x} \to \underline{x}') \leq E[D^{d^2(\underline{x},\underline{x}')}] = E\left\{\exp\left[\frac{-d^2(\underline{x}, \underline{x}')}{8\sigma^2}\right]\right\} \tag{13}$$

where $\sigma^2 = (2n\overline{E_b}/N_0)^{-1}$ and

$$d^2(\underline{x}, \underline{x}') = \begin{cases} \sum_{k\in\eta} \rho_k^2|x_k - x_k'|^2, & \text{ideal CSI} \\ \sum_{k\in\eta} 4\lambda(\rho_k - \lambda)|x_k - x_k'|^2, & \text{no CSI.} \end{cases} \tag{14}$$

Using the transfer function method [13], we can show that P_b for the two-state code analyzed in [11] is upperbounded by

$$P_b \leq \frac{1}{2n}\left.\frac{\partial T(D,I)}{\partial I}\right|_{I=1} = \frac{ab}{2(1-a)^2} \tag{15}$$

where

$$T(D,I) = \frac{Iab}{1-Ia} \tag{16a}$$

$$a = \begin{cases} E(D^{\rho^2\delta_1^2}), & \text{ideal CSI} \\ D^{-4\lambda^2\delta_1^2}E(D^{4\lambda\rho\delta_1^2}), & \text{no CSI} \end{cases} \tag{16b}$$

$$b = \begin{cases} E(D^{\rho^2\delta_2^2}), & \text{ideal CSI} \\ D^{-4\lambda^2\delta_2^2}E(D^{4\lambda\rho\delta_2^2}), & \text{no CSI} \end{cases} \tag{16c}$$

$\delta_1^2 = 2, \delta_2^2 = 4$ are the squared Euclidean distances between different pairs of signal points [see Fig. 2(a)] and ρ is a r.v.,

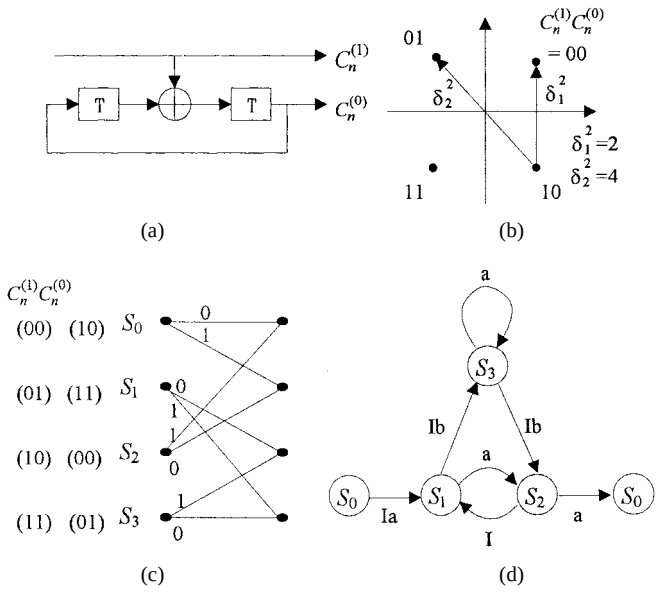

Fig. 3. (a) Encoder of four states, rate 1/2, and 4PSK code. (b) Signal constellation and squared Euclidean distance. (c) Trellis diagram of four states and (d) the corresponding signal flow graph.

which has the same distribution as ρ_k of (8). For the four-state rate 1/2 4PSK GUC code shown in Fig. 3(a)–(c), the corresponding transfer function is given by

$$T(D,I) = I^2a^2\frac{a-a^2+I^2b^2}{1-2a+a^2-I^2b^2} \tag{17}$$

and the BEP is upperbounded by

$$P_{b_2} \le \frac{1}{2n}\frac{\partial T(D,I)}{\partial I}\bigg|_{I=1} = \frac{f_1(a,b)}{2(1-2a+a^2-b^2)^2} \tag{18}$$

where

$$f_1(a,b) = 2a^3-6a^4+6a^5-2a^6+4a^2b^2-8a^3b^2+4a^4b^2 - 2a^2b^4.$$

For QRC's, we can use the modified transfer function method to obtain similar BEP upperbounds [13] [2]. The four-state rate 2/3 8PSK code analyzed in [2] is an example of QRC. It can be shown that the associated modified transfer function is given by

$$T(D,I) = \frac{f_2(I,a,b,c,d)}{1-I^2c-Ia-Id-I^2d-I^3c^2/2+I^2ad+I^3d^2/2} \tag{19}$$

where

$$\begin{aligned} f_2(I,a,b,c,d) &= I^2ac+Ibc+I^2ad+Iab+I^3ac^2-I^3bc^2/2 \\ &\quad -I^2abc+I^2b^2c/2-I^3ad^2-I^2abd+I^3d^2b/2 \\ &\quad +I^2b^2d/2-I^4a^2c^2+I^4ac^2d \end{aligned} \tag{20}$$

$$c = \begin{cases} E(D^{\rho^2\delta_3^2}), & \text{ideal CSI} \\ D^{-4\lambda^2\delta_3^2}E(D^{4\lambda\rho\delta_3^2}), & \text{no CSI} \end{cases} \tag{21a}$$

$$d = \begin{cases} E(D^{\rho^2\delta_4^2}), & \text{ideal CSI} \\ D^{-4\lambda^2\delta_4^2}E(D^{4\lambda\rho\delta_4^2}), & \text{no CSI} \end{cases} \tag{21b}$$

and $\delta_3^2 = 2-\sqrt{2}, \delta_4^2 = 2+\sqrt{2}$ are two other (besides δ_1 and δ_2) squared Euclidean distances between candidate signal points. A BEP upperbound for QRC can also be obtained in a manner similar to the GUC case. In summary, the BEP performance of both GUC and QRC can be evaluated by using either the transfer function or the modified transfer function associated with these codes. The effect of the channel characteristic is reflected in the parameters a–d, defined in (16b), (16c), (21a), and (21b), respectively. Therefore, to calculate the BEP upperbound for either GUC or QRC, we need only to compute the values of these parameters.

III. BEP Bounds

Equation (7) and the following two identities are needed in the calculation of BEP bounds for the trellis codes discussed in Section II

$$\begin{aligned} &J_2(\alpha,h,x,y) \\ &\quad \stackrel{\text{def}}{=} \int_0^\infty xh^2z\exp\left\{-\left[\alpha z^2+\frac{x(h^2z^2+y^2)}{2}\right]\right\} \\ &\qquad \times I_0(xhyz)\,dz \\ &\quad = \frac{1}{1+2\alpha/(xh^2)}\exp\left(-\frac{\alpha y^2/h^2}{1+2\alpha/(xh^2)}\right). \end{aligned} \tag{22}$$

$$\begin{aligned} &J_3(\alpha,h,x,y) \\ &\quad \stackrel{\text{def}}{=} \int_0^\infty xh^2z\exp\left\{-\left[4\alpha z+\frac{x(h^2z^2+y^2)}{2}\right]\right\} \\ &\qquad \times I_0(xhyz)\,dz \\ &\quad = e^{-xy^2/2}\left\{1-\frac{1}{\sqrt{\pi}}\int_0^\pi\sqrt{\frac{x}{2}}\,f(\theta)e^{xf^2(\theta)/2}\right. \\ &\qquad \left.\times\,\text{erfc}\,[\sqrt{x/2}f(\theta)]\,d\theta\right\} \end{aligned} \tag{23}$$

where $f(\theta) = 4\alpha/(xh) - y\cos\theta$. The last equation is derived in the Appendix, and J_2 follows directly from [14, (11.4.29)].

A. Performance with Ideal Channel State Information (CSI)

1) Mixed Model of the First Kind: For the case when the received amplitude has a pdf given by (6a), the corresponding parameters a–d can be computed via

$$\begin{aligned} E_{\rho_1}(D^{\rho_1^2\beta}) &= (1-A)E_{\text{Rice}}(D^{\rho_1^2\beta};2c_0,h_1,1) \\ &\quad + AE_{\text{Ray/Ln}}(D^{\rho_1^2\beta}) \end{aligned} \tag{24}$$

where β represents one of the squared Euclidean distances (i.e., $\delta_1^2,\delta_2^2,\delta_3^2$, and δ_4^2) defined in the last section, $E_{\text{Rice}}(x(\rho);a,b,c)$ represents the expectation of $x(\rho)$ taken with respect to the pdf $P_{\text{Rice}}(\rho;a,b,c)$, and $E_{\text{Ray/Ln}}(x)$ is the expectation of x taken with respect to the Rayleigh/lognormal part of (6a). We can easily show that the first expectation on the right-hand side of the above equation is

$$\begin{aligned} &E_{\text{Rice}}(D^{\rho_1^2\beta};2c_0,h_1,1) \\ &\quad = \frac{1}{1+g\beta/(c_0h_1^2)}\exp\left[\frac{-g\beta/h_1^2}{1+g\beta/(c_0h_1^2)}\right] \end{aligned} \tag{25}$$

where $g = n\overline{E}_b/4N_0$. The other expectation can be evaluated as follows:

$$\begin{aligned} E_{\mathrm{Ray/Ln}}(D^{\rho_1^2\beta}) &= \int_0^\infty \exp(-g\beta\rho_1^2)\int_0^\infty \frac{2h_1^2\rho_1}{S_0}\exp\left(-\frac{h_1^2\rho_1^2}{S_0}\right) \\ &\quad \times P_{\mathrm{Ln}}(S_0)\,dS_0\,d\rho_1 \\ &= \int_0^\infty \frac{1}{1+\beta S_0 g/h_1^2} P_{\mathrm{Ln}}(S_0)\,dS_0 \\ &= \frac{10}{\sigma\ln 10\sqrt{2\pi}}\left\{\frac{\ln 10\sqrt{2\pi\sigma^2}}{10} - \int_0^\infty \frac{1}{S_0+h_1^2/(\beta g)} \right. \\ &\quad \left. \cdot \exp\left[-\frac{(10\log S_0-\mu_0)^2}{2\sigma^2}\right] dS_0\right\}. \end{aligned} \tag{26}$$

The second equation in the above derivation is obtained by the change of variable $h_1^2\rho_1^2/S_0 = t^2$. Using the expansions

$$(u+v)^{-1} = \begin{cases} v^{-1}\sum_{n=0}^{\infty}\left(-\frac{u}{v}\right)^n, & \text{for } \left|\frac{u}{v}\right|<1 \\ u^{-1}\sum_{n=0}^{\infty}\left(-\frac{v}{u}\right)^n, & \text{for } \left|\frac{u}{v}\right|>1 \end{cases} \tag{27}$$

and the change of variable $10\log S_0 = x$, we can show

$$\begin{aligned} E_{\mathrm{Ray/Ln}}(D^{\rho_1^2\beta}) &= 1 - \frac{1}{2}\exp\left[-\left(\frac{\mu_0}{\sqrt{2}\sigma} - \frac{\sqrt{50}}{\sigma}\log\frac{h_1^2}{\beta g}\right)^2\right] \\ &\quad \times \sum_{n=0}^{\infty}\{(-1)^n[\exp(x_n^2)\operatorname{erfc}(x_n) + \exp(y_n^2)\operatorname{erfc}(y_n)]\} \end{aligned} \tag{28}$$

where

$$x_n = \frac{10\log\left(\frac{h_1^2}{\beta g}\right) - \left(\mu_0 - \sigma^2 n\frac{\ln 10}{10}\right)}{\sqrt{2}\sigma}$$

$$y_n = \frac{\mu_0 + \sigma^2(n+1)\frac{\ln 10}{10} - 10\log\left(\frac{h_1^2}{\beta g}\right)}{\sqrt{2}\sigma}.$$

This series expansion is very useful for it provides a computing algorithm that is more efficient than that of (26). Using the rational Chebyshev approximation proposed by Cody [15], we can accurately and efficiently compute the terms $e^{x^2}\operatorname{erfc}(x)$. Numerical results indicate that for all cases of interest, less than 20 terms are needed in the above expansion in order to obtain the required accuracy.

2) Mixed Model of the Second Kind: Similar to the previous case, we have the decomposition

$$\begin{aligned} E_{\rho_2}(D^{\rho_2^2\beta}) &= (1-A)E_{\mathrm{Rice}}(D^{\rho_2^2\beta}; k, h_2, \sqrt{2}) \\ &\quad + AE_{Rice/Ln}(D^{\rho_2^2\beta}) \end{aligned} \tag{29}$$

in which

$$\begin{aligned} E_{\mathrm{Rice}}(D^{\rho_2^2\beta}; k, h_2, \sqrt{2}) &= \frac{1}{1+2g\beta/(kh_2^2)}\exp\left(\frac{-2g\beta/h_2^2}{1+2g\beta/(kh_2^2)}\right) \end{aligned} \tag{30}$$

and

$$\begin{aligned} E_{\mathrm{Rice/Ln}}(D^{\rho_2^2\beta}) &= \int_0^\infty\int_0^\infty \frac{1}{z}\exp(-g\beta\rho_2^2)\frac{8.686h_2^2}{b_0\sqrt{2\pi}} I_0(\overline{k}\rho h_2 z) \\ &\quad \times \exp\left[-\frac{(20\log z - m)^2}{2b_0^2} - \frac{\overline{k}(\rho^2h_2^2+z^2)}{2}\right] dz\,d\rho \\ &= \frac{8.686}{b_0\sqrt{2\pi}}\int_0^\infty \frac{1}{z}\exp\left[-\frac{(20\log z - m)^2}{2b_0^2}\right] \\ &\quad \times J_2(g\beta, h_2, \overline{k}, z)\,dz. \end{aligned} \tag{31}$$

$E_{\mathrm{Rice/Ln}}(x)$ is the expectation of x taken with respect to the Rician/lognormal part of (6b). Substituting $\beta = 2, 4, 2-\sqrt{2}$ or $2+\sqrt{2}$ in the appropriate Chernoff bound equations derived above, we then obtain the associated BEP upperbounds.

B. Performance without CSI

1) Mixed Model of the First Kind: As with the perfect CSI case, we have the decomposition

$$\begin{aligned} E_{\rho_1}(D^{4\lambda\beta\rho_1}) &= (1-A)E_{\mathrm{Rice}}(D^{4\lambda\beta\rho_1}; 2c_0, h_1, 1) \\ &\quad + AE_{\mathrm{Ray/Ln}}(D^{4\lambda\beta\rho_1}). \end{aligned} \tag{32}$$

It can be shown that

$$\begin{aligned} E_{\mathrm{Rice}}(D^{4\lambda\beta\rho_1}; 2c_0, h_1, 1) &= J_3(g\lambda\beta, h_1, 2c_0, 1) \\ &= e^{-c_0}\left[1 - \frac{1}{\sqrt{\pi}}\int_0^\pi \sqrt{c_0}\theta_1 e^{c_0\theta_1^2}\operatorname{erfc}(\sqrt{c_0}\theta_1)\,d\theta\right] \end{aligned} \tag{33}$$

where

$$\theta_1 = 2g\lambda\beta/(c_0h_1) - \cos\theta$$

and

$$\begin{aligned} E_{\mathrm{Ray/Ln}}(D^{4\lambda\beta\rho_1}) &= \int_0^\infty\int_0^\infty \exp(-4\lambda g\beta\rho_1)\frac{2h_1^2\rho_1}{S_0}\exp\left(-\frac{h_1^2\rho_1^2}{S_0}\right) \\ &\quad \times P_{\mathrm{Ln}}(S_0)\,d\rho_1\,dS_0 \\ &= \int_0^\infty J_3\left(g\lambda\beta, h_1, \frac{2}{S_0}, 0\right)P_{\mathrm{Ln}}(S_0)\,dS_0. \end{aligned} \tag{34}$$

The last equation can be further simplified to

$$\begin{aligned} E_{\mathrm{Ray/Ln}}(D^{4\lambda\beta\rho_1}) &= 1 - \sqrt{\pi}\int_0^\infty \theta_2 e^{\theta_2^2}\operatorname{erfc}(\theta_2)P_{\mathrm{Ln}}(S_0)\,dS_0 \end{aligned} \tag{35}$$

where $\theta_2 = \lambda\beta\sqrt{S_0}2g/h_1$.

2) Mixed Model of the Second Kind: For the decomposition

$$\begin{aligned} E_{\rho_2}(D^{4\lambda\beta\rho_2}) &= (1-A)E_{\mathrm{Rice}}(D^{4\lambda\beta\rho_2}; k, h_2, \sqrt{2}) \\ &\quad + AE_{\mathrm{Rice/Ln}}(D^{4\lambda\beta\rho_2}) \end{aligned} \tag{36}$$

the first term on the right-hand side is given by

$$\begin{aligned} &E_{\text{Rice}}(D^{4\lambda\beta\rho_2}; k, h_2, \sqrt{2}) \\ &\quad = \int_0^\infty k\rho_2 h_2^2 \exp(-4g\lambda\beta\rho_2) \exp[-k(1+.5\rho_2^2 h_2^2)] \\ &\qquad \times I_0(\sqrt{2}k\rho_2 h_2)\, d\rho_2 \\ &\quad = J_3(g\lambda\beta, h_2, k, \sqrt{2}). \end{aligned} \tag{37}$$

The substitution $h = h_2,\ x = \overline{k}$, and $y = z$ leads to

$$\begin{aligned} &E_{\text{Rice/Ln}}(D^{4\lambda\beta\rho_2}) \\ &\quad = \int_0^\infty \exp(-4g\lambda\beta\rho_2) \frac{8.686\overline{k}\rho_2 h_2^2}{b_0\sqrt{2\pi}} \\ &\qquad \times \int_0^\infty \frac{1}{z} \exp\left[-\frac{(20\log z - m)^2}{2b_0^2} - \frac{\overline{k}(\rho_2^2 h_2^2 + z^2)}{2}\right] \\ &\qquad \times I_0(\overline{k}\rho_2 z h_2)\, dz\, d\rho_2 \\ &\quad = \int_0^\infty \frac{8.686}{b_0\sqrt{2\pi}z} \exp\left[-\frac{(20\log z - m)^2}{2b_0^2}\right] \\ &\qquad \times J_3(g\lambda\beta, h_2, \overline{k}, z)\, dz. \end{aligned} \tag{38}$$

IV. Asymptotic Analysis and Design Criteria

In this section, we study the asymptotic BEP behaviors of TCM/MPSK systems. The usefulness of asymptotic analysis lies in the fact that it can tell us which parameter(s) of the code used dominate the system performance when $\overline{E}_b/N_0$ becomes sufficiently large. Thus, a judicious choice of the trellis code to be used is made possible. In [1], it was shown that in a Rician fading environment

$$P_b \simeq \frac{1}{b} C \left(\frac{(1+K)e^{-K}}{\overline{E}_s/N_0}\right)^L, \qquad \overline{E}_s/N_0 \gg K \tag{39}$$

where b is a constant, C is a function of the weight distribution of the code, K is the ratio of the power in LOS plus specular component to that in the diffuse component, and L is the length of the shortest error-event path, defined as [12] the error-event path whose Hamming distance to the correct path is the smallest amongst all possible error events. We shall show that similar asymptotic performance bounds for the two mixed channels under consideration also exist. For all the derivation in this section, $g \gg 1$ is assumed. Let us consider the mixed model of the first kind to begin with. For a TCM/MPSK scheme to operate in such a channel with ideal CSI reception, we have from (25)

$$E_{\text{Rice}}(D^{\rho_1^2\beta}; 2c_0, h_1, 1) \simeq e^{-c_0} \frac{c_0 h_1^2}{g\beta} \tag{40}$$

and from (26)

$$\begin{aligned} &E_{\text{Ray/Ln}}(D^{\rho_1^2\beta}) \\ &\quad \simeq \int_0^\infty \frac{h_1^2}{\beta S_0 g} P_{\text{Ln}}(S_0)\, dS_0 \\ &\quad = \frac{h_1^2}{\beta g} \exp\left[\frac{\sigma^2}{2}\left(\frac{\ln 10}{10}\right)^2 - \mu_0 \frac{\ln 10}{10}\right]. \end{aligned} \tag{41}$$

Defining

$$\begin{aligned} c_1 = &(1-A)e^{-c_0} c_0 h_1^2 + A h_1^2 \\ &\cdot \exp\left[\frac{\sigma^2}{2}\left(\frac{\ln 10}{10}\right)^2 - \mu_0 \frac{\ln 10}{10}\right] \end{aligned} \tag{42}$$

we can write

$$E_{\rho_1}(D^{\rho_1^2\beta}) \simeq \frac{c_1}{g\beta}. \tag{43}$$

When CSI is not available, θ_1 in (33) approaches $2g\lambda\beta/(c_0 h_1)$ as g becomes sufficiently large. Invoking the asymptotic expansion

$$\operatorname{erfc}(\alpha) \simeq \frac{e^{-\alpha^2}}{\sqrt{\pi}\alpha}\left(1 - \frac{1}{2\alpha^2}\right)$$

we obtain

$$E_{\text{Rice}}(D^{4\lambda\beta\rho_1}; 2c_0, h_1, 1) \simeq \frac{e^{-c_0} c_0 h_1^2}{8g^2\lambda^2\beta^2}. \tag{44}$$

Note that $P_{\text{Ln}}(S_0)$ is negligibly small when S_0 is close to zero, and, therefore, errors incurred by approximating other parts of the integrand in the small S_0 region contribute very little to the integration. This observation and the asymptotic expansion of $\operatorname{erfc}(\alpha)$ lead to

$$\begin{aligned} &E(D^{4\lambda\beta\rho_1})_{\text{Ray/Ln}} \\ &\quad \simeq \frac{h_1^2}{8\lambda^2\beta^2 g^2} \exp\left[\frac{\sigma^2}{2}\left(\frac{\ln 10}{10}\right)^2 - \mu \frac{\ln 10}{10}\right]. \end{aligned} \tag{45}$$

From (44) and (45), we have

$$E_{\rho_1}(D^{4\lambda\beta\rho_1}) \simeq \frac{c_1'}{\beta^2 g^2 \lambda^2} \tag{46}$$

where

$$\begin{aligned} c_1' = &\frac{(1-A)e^{-c_0} c_0 h_1^2}{8} + \frac{A h_1^2}{8} \\ &\cdot \exp\left[\frac{\sigma^2}{2}\left(\frac{\ln 10}{10}\right)^2 - \mu \frac{\ln 10}{10}\right]. \end{aligned} \tag{47}$$

Next, let us consider the mixed model of the second kind. For the ideal CSI case, we have

$$E_{\rho_2}(D^{\rho_2^2\beta}) \simeq \frac{c_2}{g\beta} \tag{48}$$

where

$$\begin{aligned} c_2 = &(1-A)\frac{k e^{-k} h_2^2}{2} + A\frac{\overline{k} h_2^2}{2}\left\{\frac{8.686}{\sqrt{2\pi}b_0} \times \int_0^\infty \frac{1}{z} \right. \\ &\left. \cdot \exp\left[-\frac{(20\log z - m)^2}{2b_0^2}\right] \exp\left(-\overline{k}\frac{z^2}{2}\right) dz\right\}. \end{aligned} \tag{49}$$

The corresponding aymptotic form when there is no CSI is

$$E_{\rho_2}(D^{4\lambda\beta\rho_2}) \simeq \frac{c_2'}{\beta^2 g^2 \lambda^2} \tag{50}$$

where

$$c_2' = \left(\frac{h_2}{4}\right)^2 \left[(1-A)ke^{-k} + A\bar{k}\int_0^\infty \frac{8.686}{b_0\sqrt{2\pi}z} \times \exp\left[-\frac{(20\log z - m)^2}{2b_0^2}\right] e^{(-\bar{k}z^2/2)}\, dz\right]. \quad (51)$$

Summarizing, we conclude that

$$E_{\rho_i}(D^{\rho_i^2\beta}) \simeq \frac{c_i}{g\beta}, \qquad i = 1, 2, \quad \text{(ideal CSI)} \quad (52)$$

and

$$E_{\rho_j}(D^{4\lambda\beta\rho_j}) \simeq \frac{c_j'}{g^2\beta^2\lambda^2}, \qquad j = 1, 2 \quad \text{(no CSI)}. \quad (53)$$

From (13) and (14), the pairwise error probability is thus bounded by

$$P(\underline{x} \to \underline{x}') \le \begin{cases} \prod_{i\in\eta} \dfrac{c_i}{g|x_i - x_i'|^2}, & \text{ideal CSI} \\ \prod_{i\in\eta} \dfrac{c_j' \exp(4ng\lambda^2|x_i - x_i'|^2)}{g^2\lambda^2|x_i - x_i'|^4}, & \text{no CSI} \end{cases} \quad (54)$$

where η is the set of all i for which $x_i \neq x_i'$. Substituting (54) into (12) and taking into account the fact that $g \gg 1$, we obtain

$$P_{b_i} \le \begin{cases} \dfrac{1}{2n}\left(\dfrac{c_i}{g}\right)^L M, & \text{ideal CSI} \\ \dfrac{1}{2n}\left(\dfrac{c_j'}{g^2}\right)^L [\min_{\lambda>0} N(\lambda)], & \text{no CSI} \end{cases} \quad (55a)$$

where

$$M = \sum_{\underline{x_L}} P(\underline{x_L}) \sum_{\underline{x_L}'} \frac{a(\underline{x_L}, \underline{x_L}')}{l_1(\underline{x_L}, \underline{x_L}')} \quad (55b)$$

$$N(\lambda) = \frac{1}{\lambda^{2L}} \sum_{\underline{x_L}} P(\underline{x_L}) \times \sum_{\underline{x_L}'} \frac{a(\underline{x_L}, \underline{x_L}')}{l_1(\underline{x_L}, \underline{x_L}')} \exp(4ng\lambda^2 l_2(\underline{x_L}, \underline{x_L}')) \quad (55c)$$

and $\underline{x_L} = (x_1, x_2, \cdots, x_L)$ is a transmitted code word of length L and $\underline{x_L}' = (x_1', x_2', \cdots, x_L')$ is any other length L code word, where x_i and x_i' are MPSK signals. Furthermore

$$l_1(\underline{x_L}, \underline{x_L}') = \sum_{i=1}^{L} |x_i - x_i'|^2 \quad (56a)$$

$$l_2(\underline{x_L}, \underline{x_L}') = \prod_{i=1}^{L} |x_i - x_i'|^2. \quad (56b)$$

Note that for the no-CSI case, the corresponding Chernoff bound is to be obtained by minimizing $N(\lambda)$ over λ. It can be shown that the optimal values for λ are in proportion to $1/\sqrt{g}$, and, therefore, P_{b_i}'s are proportional to g^{-L} for both CSI and no-CSI cases.

From the above discussion, we know that the BEP bound is inversely proportional to g^L. Furthermore, the BEP is dominated by two factors: 1) the length of the shortest error-event path and 2) the product of all the squared Euclidean distances between paths with this (Hamming) length and the correct path, or equivalently, the number of nearest neighbors. The code rate $n/n+1$ also plays a role in the asymptotic bounds.

TABLE I
CHANNEL PARAMETERS FOR THE MIXED MODEL OF THE FIRST KIND

case	environment	A	C_0(dB)	μ_0(dB)	σ(dB)
lu1	highway	0.002	17.3	-13.8	2
lu2	highway	0.19	17.4	-8.1	4.2

TABLE II
CHANNEL PARAMETERS FOR THE MIXED MODEL OF THE SECOND KIND

case	A	k (dB)	$\bar{k}$ (dB)	m (dB)	b_0 (dB)
st1	0.67	20	20	-3.1	0.9
st2	0.6	10	20	-9.93	1.36
lo	1	-	12	-34	7

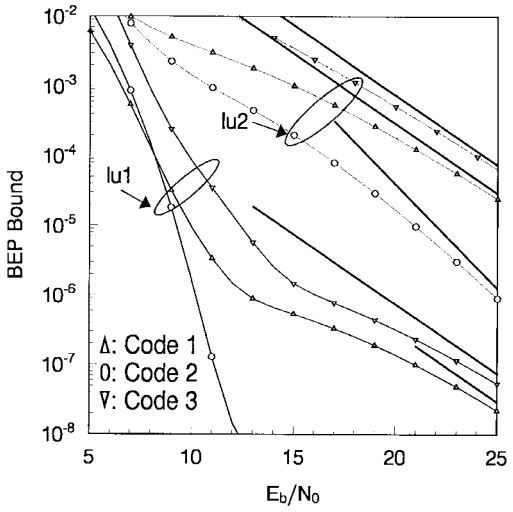

Fig. 4. BEP bounds for receivers with ideal CSI in various mixed channels of the first kind; asymptotic bounds are represented by boldface lines.

V. NUMERICAL RESULTS AND DISCUSSIONS

We will refer to the two-state rate 1/2, 4PSK code mentioned in Section II as Code 1, the four-state rate 1/2 4PSK code as Code 2, and the four-state rate 2/3 8PSK code as Code 3. The channel parameters used in our simulation are listed in Tables I and II, respectively. Table I provides the parameter values for the mixed channel of the first kind, and Table II are those for the Barts and Stutzman model.

Figs. 4–5(b) show the BEP bounds with ideal CSI, while Figs. 6–7(b) depict those without CSI. As expected, the receiver with ideal CSI outperforms that without. The extent of the improvement depends on channel condition and the

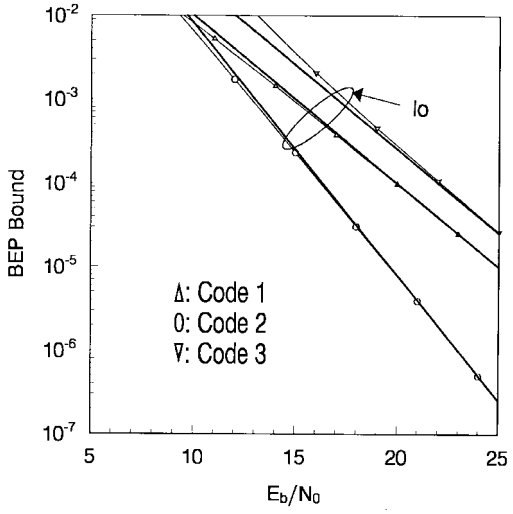

(a)

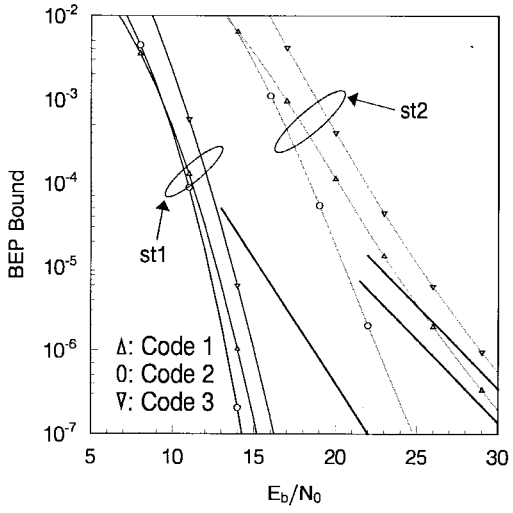

(b)

Fig. 5. (a) BEP bounds for receivers with ideal CSI in various mixed channels of the second kind; asymptotic bounds are represented by boldface lines. (b) BEP bounds for receivers with ideal CSI in various mixed channels of the second kind; asymptotic bounds are represented by boldface lines.

trellis code used. The better the channel condition and the trellis code used are, the less the improvement becomes. When Code 2 is used in the mixed channel labeled as "st1," the improvement is less than 1 dB when the BEP bound $= 10^{-7}$. On the other hand, for Code 3 and channel condition "st2," the improvement brought about by perfect CSI is 2.5 dB when BEP bound $= 1.1 \times 10^{-5}$. On the average, the improvement of $\overline{E}_b/N_0$ is about 1.5 dB when ideal CSI is provided. Substituting (52) and (53) into the defining equations for a–d and then the BEP bounds for P_{b_1}, P_{b_2}, and P_{b_3} gives the corresponding asymptotic performance formula. We depict some of these curves in Figs. 4–7 for the purpose of comparison. These asymptotic performance curves indicate that the analysis presented in the last section is indeed valid.

Recall that we have found that the BEP bounds are dominated by three factors when signal-to-noise ratio is sufficiently high. Let us examine more closely how these three factors affect the asymptotic behavior of the three codes we have

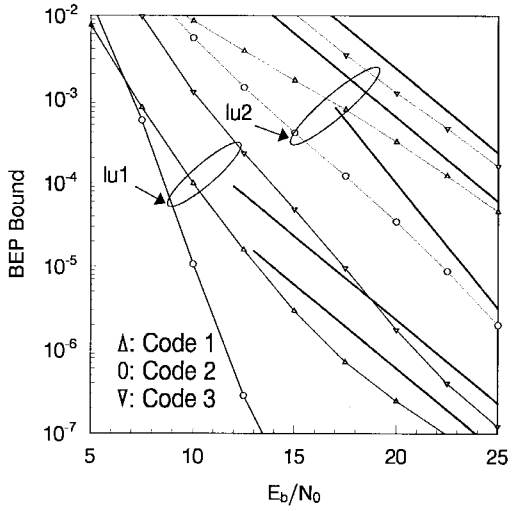

Fig. 6. BEP bounds for receivers without ideal CSI in various mixed channels of the first kind; asymptotic bounds are represented by boldface lines.

selected. Applying long division on the BEP bounds for P_{b_i}'s, followed by some algebraic manipulations, we obtain

$$P_{b_1} \leq (ab + \text{higher order terms})/2 \tag{57a}$$

$$P_{b_2} \leq (2a^3 + \text{higher order terms})/2 \tag{57b}$$

and

$$P_{b_3} \leq (2ac + bc + 2ad + ab + \text{higher order terms})/4 \tag{57c}$$

where the order of a given term is defined as the sum of the exponents for a, b, c, or d appearing in that term. The order of the lowest order term in a BEP bound equation is equal to the length of the shortest error-event path. The above three inequalities indicate that Code 2 will outperform the other two codes asymptotically since the lowest order term in its BEP bound equation has the largest exponent among the three BEP bounds. Our simulation confirms this observation. Substituting the values of a, b, c, and d we have obtained in the above inequalities and neglecting the higher order terms, we find that

$$P_{b_1} \leq \begin{cases} \dfrac{c_i^2}{g_1^2}, & \text{ideal CSI} \\ \dfrac{2c_j'^2 \exp(6g_1\lambda^2)}{g_1^4\lambda^4}, & \text{no CSI} \end{cases} \tag{58a}$$

$$P_{b_2} \leq \begin{cases} \dfrac{8c_i^3}{g_1^3}, & \text{ideal CSI} \\ \dfrac{64c_j'^3 \exp(6g_1\lambda^2)}{g_1^6\lambda^6}, & \text{no CSI} \end{cases} \tag{58b}$$

$$P_{b_3} \leq \begin{cases} \dfrac{c_i^2}{g_1^2}\dfrac{19+\sqrt{2}}{8}, & \text{ideal CSI} \\ \dfrac{4c_j'^2}{g_1^4\lambda^4}\left[\dfrac{e^{[2g_1\lambda^2(4-\sqrt{2})]}}{4(2-\sqrt{2})^2} + \dfrac{e^{[2g_1\lambda^2(6-\sqrt{2})]}}{16(2-\sqrt{2})^2}\right. & \\ \qquad \left. + \dfrac{e^{[2g_1\lambda^2(4+\sqrt{2})]}}{4(2+\sqrt{2})^2} + \dfrac{e^{(12g_1\lambda^2)}}{64}\right], & \text{no CSI.} \end{cases} \tag{58c}$$

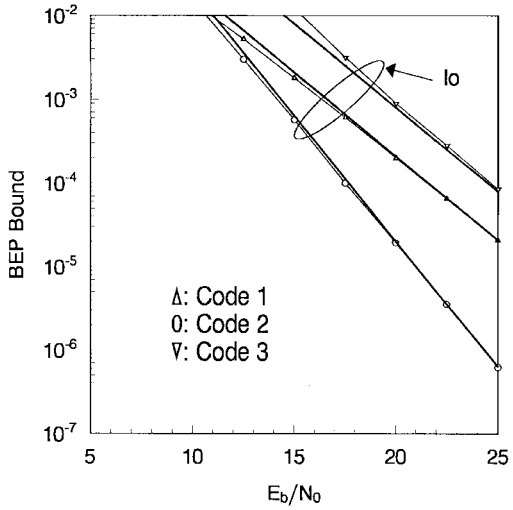

(a)

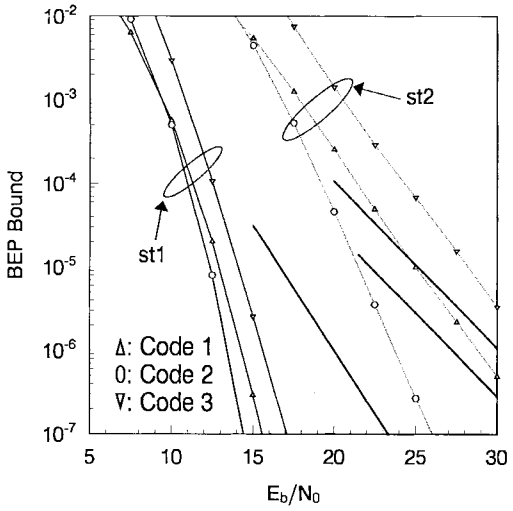

(b)

Fig. 7. (a) BEP bounds for receivers without ideal CSI in various mixed channels of the second kind; asymptotic bounds are represented by boldface lines. (b) BEP bounds for receivers without ideal CSI in various mixed channels of the second kind; asymptotic bounds are represented by boldface lines.

Solving the λ's that satisfy the Chernoff bound condition leads to $\lambda = 1/\sqrt{3g_1}$, $1/\sqrt{2g_1}$, and $.535/\sqrt{g_1}$ for Codes 1, 2, and 3, respectively. The BEP bounds for the no-CSI case become

$$P_{b_1} \leq 133 c_j'^2/g_1^2 \tag{59a}$$

$$P_{b_2} \leq 10\,283.8 c_j'^3/g_1^3 \tag{59b}$$

$$P_{b_3} \leq 505.5 c_j'^2/g_1^2 \tag{59c}$$

where $g_1 = \overline{E}_b/N_0$. The corresponding values for c_j''s can be calculated once the channel parameters are known. Substituting c_j''s into the above inequalities, we have the logarithmic slopes $-\log(P_{b_i})/10\log(\overline{E}_b/N_0) \simeq 2(i=1,3)$ and $3(i=2)$. This is consistent with what (55a) and (55b) have predicted. Similarly, it is found that the asymptotic coding gain of Code 1 with respect to Code 2 is $5\log(19+\sqrt{2})/8 = 2$ dB for the ideal CSI case and $5[\log(505.5) - \log(133)] = 2.89$ dB for the no-CSI case. Our simulation results indicate that these estimations are very reliable when $\overline{E}_b/N_0$ is above 30 dB.

VI. Conclusion

We have presented the BEP bounds for trellis-coded MPSK systems over two classes of mobile satellite fading channels. As mentioned before, these two classes encompass a large fraction of mobile satellite communication channels encountered in practice. One can use appropriate parameter values and accurately describe the channel under which the designed system is supposed to operate. The trellis codes analyzed here are members of GUC or QRC. They have low implementation complexity, modest error-correcting capability, and are suitable for use in a mobile satellite environments. Asymptotic BEP bounds are found, and numerical validation is provided. These bounds are similar to those obtained in simpler (Rician or Rayleigh) fading models. In other words, the key parameters that dominate the BEP behavior are the length of the shortest error-event path and the product of the squared Euclidean distance between the correct path and all the corresponding shortest-Hamming-length error-event paths.

Appendix
Derivation of (23)

$$J_3(\alpha,h,x,y) = w\int_0^\infty xh^2 z \exp\left[-4\alpha z - \frac{xh^2z^2}{2}\right] I_0(xhzy)\,dz \tag{A.1}$$

$$= w\int_0^\pi \frac{xh^2}{\pi}\int_0^\infty z \times \exp\left[-\frac{xh^2z^2}{2} - 4\alpha z + xhyz\cos\theta\right] dz\,d\theta \tag{A.2}$$

$$= w\int_0^\pi \frac{xh^2}{\pi}\int_0^\infty z\exp\left[-\frac{xh^2}{2}\left(z+\frac{4\alpha}{xh^2}-\frac{y\cos\theta}{h}\right)^2 + \frac{xh^2}{2}\left(\frac{4\alpha}{xh^2}-\frac{y\cos\theta}{h}\right)^2\right] dz\,d\theta \tag{A.3}$$

$$= w\int_0^\pi \frac{xh^2}{\pi}\int_0^\infty z\exp\left[-\frac{x}{2}(hz+f(\theta))^2 + \frac{x}{2}f^2(\theta)\right] \cdot dz\,d\theta \tag{A.4}$$

$$= w\int_0^\pi \frac{x}{\pi}\int_{\sqrt{x/2}f(\theta)}^\infty \left(\sqrt{\frac{2}{x}}r - f(\theta)\right) \times \exp\left[-r^2 + \frac{xf^2(\theta)}{2}\right]\sqrt{\frac{2}{x}}\,dr\,d\theta \tag{A.5}$$

$$= w\left\{\frac{x}{\pi}\int_0^\pi\int_{\sqrt{x/2}f(\theta)}^\infty \sqrt{\frac{2}{x}}r\exp\left[-r^2+\frac{xf^2(\theta)}{2}\right] \times \sqrt{\frac{2}{x}}\,dr\,d\theta - \frac{x}{\pi}\int_0^\pi\int_{\sqrt{x/2}f(\theta)}^\infty f(\theta) \times \exp\left[-r^2+\frac{xf^2(\theta)}{2}\right]\sqrt{\frac{2}{x}}\,dr\,d\theta\right\} \tag{A.6}$$

$$= w\left\{\frac{1}{\pi}\int_0^{\pi}\exp\left(\frac{xf^2(\theta)}{2}\right)\int_{(x/2)f^2(\theta)}^{\infty}\exp(-t)\,dt\,d\theta - \frac{\sqrt{2x}}{\pi}\int_0^{\pi}f(\theta)\exp\left(\frac{xf^2(\theta)}{2}\right) \times \int_{\sqrt{x/2}f(\theta)}^{\infty}\exp(-r^2)\,dr\,d\theta\right\} \quad \text{(A.7)}$$

$$= w\left\{1-\frac{1}{\sqrt{\pi}}\int_0^{\pi}\sqrt{\frac{x}{2}}f(\theta)\exp\left(\frac{xf^2(\theta)}{2}\right) \times \operatorname{erfc}\left(\sqrt{\frac{x}{2}}f(\theta)\right)d\theta\right\} \quad \text{(A.8)}$$

where $w = \exp(-(xy^2/2))$. In deriving (A.4), we have used the definition $f(\theta) = 4\alpha/xh - y\cos\theta$. (A.5) is obtained by the change of variable $r = \sqrt{x/2}(hz + f(\theta))$. The usefulness of this identity is threefold: 1) the integration interval is reduced from $(0,\infty)$ to $(0,\pi)$; 2) as mentioned in Section III-A-1, the integrand $e^{x^2}\operatorname{erfc}(x)$ can be very accurately and efficiently computed [15]; and 3) a simple expression of an asymptotic BEP bound can easily be derived by using the asymptotic formula for $\operatorname{erfc}(x)$.

REFERENCES

[1] E. Biglieri, D. Divsalar, P. J. McLane, and M. K. Simon, *Introduction to Trellis-Coded Modulation with Applications*. New York: Macmillan, 1991.

[2] R. G. McKay, P. J. McLane, and E. Biglieri, "Error bounds for trellis-coded MPSK on a fading mobile satellite channel," *IEEE Trans. Commun.*, vol. 39, pp. 1750–1761, Dec. 1991.

[3] J. Goldhirsh and W. J. Volgel, "Propagation effects for land mobile satellite systems: Overview of experimental and modeling results," NASA Reference Publication 1274, 1992.

[4] E. Lutz, D. Cygan, M. Dippold, F. Dolainsky, and W. Papke, "The land mobile satellite communication channel-recording, statistics, and channel model," *IEEE Tran. Veh. Technol.*, vol. 40, no. 2, pp. 375–385, 1991.

[5] C. Loo, "A statistical model for a land mobile satellite link," *IEEE Trans. Veh. Technol.*, vol. VT-34, pp. 122–127, Aug. 1985.

[6] R. M. Barts and W. L. Stutzman, "Modeling and simulation of mobile satellite propagation," *IEEE Trans. Antennas Propagat.*, vol. 40 no. 4, pp. 375–382 1992.

[7] F. I. Meno, "Mobile radio fading in Scandinavian terrain," *IEEE Trans. Veh. Technol.*, vol. VT-26, no. 4, pp. 335–340, 1977.

[8] D. O. Reudink, "Properties of mobile radio propagation above 400 MHz," *IEEE Trans. Veh. Technol.*, vol. VT-23, no. 4, pp. 143–160, 1974.

[9] W. C. Y. Lee and Y. S. Yeh, "On the estimation of the second-order statistics of log-normal fading in mobile environment," *IEEE Trans. Commun.*, vol. COM-22, p. 869, June 1974.

[10] E. Lutz, "Code and interleaver design for data transmission over fading channel," in *Proc. GLOBECOM '84*, Atlanta, GA, 1984, pp. 381–386.

[11] D. Divsalar and M. K. Simon, "Trellis coded modulation for 4800–9600 bits/s transmission over a fading mobile satellite channel," *IEEE J. Select. Areas Commun.*, vol. SAC-5, pp. 162–175, Feb. 1987.

[12] ———, "The design of trellis coded MPSK for fading channels: Performance criteria," *IEEE Trans. Commun.*, vol. 36, pp. 1004–1012, Sept. 1988.

[13] S. Benedetto, M. Mondin, and G. Montorsi, "Performance evaluation of trellis coded modulation scheme," *Proc. IEEE*, vol. 82, no. 6, pp. 833–855, 1994.

[14] M. Abramowitz and I. A. Stegun, *Handbook of Mathematical Functions*. New York: Dover, 1970.

[15] W. J. Cody, "Rational Chebyshev approximation for the error function," *Math. Comput.*, vol. 23, no. 107, pp. 631–637, July 1969.

Wen-Chang Lin was born in Yuanlin, Taiwan, on June 22, 1957. He received the B.S., M.S., and Ph.D. degrees in electronics engineering from the National Chiao Tung University, Hsinchu, Taiwan, in 1980, 1982, and 1997, respectively.

Since 1985, he has been with the Industrial Technology Research Institute (ITRI), Hsinchu, where he is engaged in several activities in the field of digital modulation and demodulation. His current research interests are in CDMA cellular systems and the DECT system.

Yu T. Su (S'81–M'83) received the B.S.E.E. degree from Tatung Institute of Technology, Taipei, Taiwan, in 1974 and the M.S. and Ph.D. degrees from the University of Southern California, Los Angeles, in 1983.

From May 1983 to September 1989, he was with LinCom Corporation, Los Angeles. He is currently a Faculty Member in the Department of Communication Engineering and the Microelectronic and Information System Research Center, National Chiao Tung University, Hsinchu, Taiwan. His present research interests are in the areas of communication theory and statistical signal processing.